Coordination/Cooperation Strategies and Optimal Zero-Forcing Precoding Design for Multi-User Multi-Cell VLC Networks

Thanh V. Pham, *Student Member, IEEE*, and Anh T. Pham, *Senior Member, IEEE*

Abstract

This paper studies multi-user multi-cell visible light communications networks in which each cell is composed of multiple LED arrays. The use of multiple LED transmitters enables each cell to support multiple users by means of precoding techniques. In such multi-user multi-cell networks, the signal for each user can be severely interfered not only by the signals that are intended to other users in the same cell, i.e., intra-cell interference, but also by the signals for users of the other cells, i.e., inter-cell interference. While intra-cell interference can be handled by the underlaying precoding scheme, it is hard to deal with the inter-cell one. The paper focuses on cell coordination/cooperation strategies and their corresponding coordinated/cooperative precoder designs as the approaches to alleviate, or possibly, to cancel out the inter-cell interference. We first derive a lower and upper bounds on the capacity of Gaussian interference channels with amplitude constraints on the input and the interference. Capitalizing on derived bounds and the zero-forcing scheme as the underlaying precoding technique, optimal coordinated/cooperative precoding designs to maximize users' sum-rate are investigated under the non-negativity and amplitude-limited constraints on the channel inputs. Comprehensive numerical results are presented to compare the performance of the considered coordination/cooperation strategies.

Index Terms

The material in this paper was presented in part at the IEEE International Conference on Communications (ICC), Paris, France, June 2017 and the IEEE Global Communications Conference (GLOBECOM), Singapore, December 2017.

Thanh V. Pham and Anh T. Pham are with the Computer Communications Lab., The University of Aizu, Aizuwakamatsu 965-8580, Japan (e-mail: d8182105@u-aizu.ac.jp; pham@u-aizu.ac.jp).

VLC, multi-user multi-cell VLC, zero-forcing precoding, cell coordination/cooperation, coordinated/cooperative precoding.

I. INTRODUCTION

The exponentially increasing demand for high data-rate wireless communications has been posing several challenges to the existing technologies. Moreover with the spectrum and power scarcity problems in radio frequency (RF) communications, there is an urgent need for a new wireless technology. The last decade has witnessed a tremendous research effort on visible light communications (VLC), which is regarded as a promising candidate to address the aforementioned issues [1]–[4]. Capitalizing on the massive deployment of light emitting diodes (LEDs), VLC is also expected to play an important role in the future of ubiquitous networks [5], [6]. To open the road for commercialization, VLC has also been standardized for wireless personal area networks (WPANs) in IEEE 802.15.7 [7], [8]. The expected ubiquity of the future VLC means that it should be able to support multiple users in large public areas, such as supermarkets, stations or airports. Considering the fact that the illuminating coverage of LEDs is limited, this requirement essentially makes multi-cell configuration an inevitable progression in the development of future VLC networks.

Initial research on multi-cell VLC networks focused on the model composed of small optical atto-cells, where each individual cell is illuminated by a LED array (LED luminaire) which is also known as an optical Access Point (AP). Nevertheless, if the same frequency resources are used across all cells, the inter-cell interference, which severely degrades the signal to interference plus noise ratio (SINR) of cell-edge users, is inevitable. As a result, methods for mitigating or eliminating the impact of inter-cell interference are of particular importance in the design of multi-cell VLC networks. In fact, several approaches have been proposed to deal with the problem. In [9], the concept of joint transmission (JT) in RF was adapted to the atto-cell VLC networks. The proposed JT scheme was developed based on a specific structure of the APs in which each AP was composed of multiple clusters with different beam directions. Two transmission regions, namely: single point transmission region and multipoint transmission region were then defined according to the position of the user. Users within the single point transmission region were served by a cluster by means of Orthogonal Frequency Division Multiplexing (OFDM). On the other hand, users in the multipoint transmission region were served by multiple clusters from different APs and the traditional frequency-partitioning approach

was utilized to avoid the inter-cell interference. The same authors in [10] proposed a fractional frequency reuse (FFR) strategy to avoid the inter-cell interference at the expense of reduced bandwidth efficiency. Furthermore, the atto-cell configuration with FFR limits the mobility of user since switching frequencies during user movement degrades the user experience, which is a critical measure to some quality-sensitive services, such as video streaming and voice over IP (VoIP) [11]. Aside from the frequency partition approach, several works focused on cooperative transmission and signal design. Specifically, a cooperative transmission and reception based on On-Off Keying (OOK) and Pulse Position Division Multiplexing (PPDM) have been proposed [12]. While enabling a relatively simple transmission scheme, the proposed method required the receiver to have some information about the transmitter, which increases the complexity of the system. Efficient signal designs based on phase-shifted superposition and time superposition to mitigate interference have also been recently explored in [13], [14]. These design, however, still compromised the system bandwidth efficiency.

Due to the fact that commercial LEDs have limited modulation bandwidth (up to 20 MHz for the popular phosphorescent LEDs), the unity frequency reuse (UFR) strategy is more favorable as it allows users to make use of the full available spectrum. Advanced signal processing techniques then can be employed at the transmitters to alleviate the impact of inter-cell interference together with improving user mobility. The concept of transmit precoding, i.e., beamforming in multi-user RF therefore has been recently adopted to multi-user VLC systems. This approach essentially combines neighboring atto-cells into a larger mutli-AP cell, which is termed as coordinated multipoint (CoMP) cell. Under specific constraints in VLC, a number of precoding techniques were thoroughly studied for this single CoMP cell configuration under different performance of interests [15]–[20].

Building upon the well-established single CoMP cell configuration, our first aim in this paper is to extend the concept to a multiple cell fashion to realize large-scale VLC networks. It should be noted that the concept of multi-cell CoMP in VLC was first introduced in [21] where the cell (cluster) formation is dynamically constructed and adjusted based on the user-centric vector transmission (UC-VT) principle (i.e., cell shapes are dependent upon user distribution). In this work, we follow the network-centric approach where the cell formation is fixed independently of user distribution. Similar to the previously studied single CoMP cell [16], the zero-forcing (ZF) precoding technique is utilized to support multiple users in one cell. Due to the above mentioned advantages of improved user mobility and enhanced bandwidth efficiency, the UFR

strategy is adopted across all CoMP cells. Consequently, desired signals for users in one cell can be severely interfered by both intra-cell and inter-cell interferences. While the intra-cell interference could be handled effectively by means of precoding techniques in much the same way as in the case of single cell, it is challenging to deal with the inter-cell one. Different from the widely used frequency partition approach in atto-cell networks, the underlaying precoding scheme used in each CoMP cell introduces another way to overcome the challenge. That is by allowing coordination and/or cooperation, e.g., coordinated/cooperative precoding design, among cells, it is possible to jointly design their precoders. The inter-cell interference, therefore, can be alleviated (or eliminated) by the coordinated/cooperative precoders.

To the best of our knowledge, our previous studies [22], [23] were the first works which concerned the multi-cell configuration and its cooperative precoding design[1]. Specifically, we considered a cooperative scheme in which cells are allowed to exchange user's channel state information (CSI) and data to each other. Based on a simple lower bound for user data-rate, the optimal cooperative ZF precoding design to maximize users sum-rate was then formulated and solved. Recently, a similar cell formation was also reported by [24]. Under the assumption that users downlink CSI could be exchanged through a backbone network among cells, a coordinated precoding scheme was proposed based on the weighted sum mean square error (WSMSE) as the performance criterion. In this paper, we further examine different strategies of cell coordination/cooperation and their corresponding coordinated/cooperative precoding designs in multi-user multi-cell VLC, namely: per cell coordinated precoding, coordinated precoding, and cooperative precoding with partial data sharing. Different from [24], the user sum-capacity is adopted as the performance metric for the precoding designs. Moreover, compared to [23], a comprehensive analysis of user date-rate will be provided as benchmarks for the optimal precoder designs. It is known that the input signal of the LEDs is amplitude constrained. Therefore, the classical Shannon capacity formula for complex and average power constrained signal is not applicable in VLC. Additionally, in our considered multi-cell system, the VLC channel is subjected to interference which is also amplitude constrained. In this work, we first derive a lower and upper bound on the channel capacity of a scalar Gaussian interference channel in which both input signal and interference are amplitude constrained. Capitalizing on the derived

[1]In this paper, we use the term multi-cell for referring to the multi-CoMP cell configuration.

bounds, the optimal ZF precoding design will be solved for each each coordinated/cooperative strategy.

The remainder of the paper is organized as follows. In Section II, we examine the scalar Gaussian interference channels with amplitude-constrained input signal and interferences. Simple lower and upper bounds of the channel capacity are provided as benchmarks for the subsequent coordinated/cooperative precoding designs. Section III describes the multi-cell VLC system model along with the precoding transmission model. In Section IV, several cell coordination/cooperation strategies are investigated. The optimal coordinated/cooperative ZF precoder design for each approach is then formulated as a convex optimization problem which can be solved efficiently by off-the-shelf optimization packages. Numerical results and comparisons among the considered coordinated/cooperative forms are given in Section V. Finally, we conclude the paper in Section VI.

Notation: The following notations are used throughout the paper. $\mathbb{R}$ indicates the real number set. Bold upper case letters denote matrices, e.g., $\mathbf{A}$. The transpose of $\mathbf{A}$ is written as $\mathbf{A}^T$ while $\mathbf{A}_{k,:}$ represents the $k-$th row vector of $\mathbf{A}$. $\mathbb{I}(\cdot;\cdot)$ and $h(\cdot)$ denote the mutual information and the differential entropy in $nats$, respectively. $\|\cdot\|_1$ and $|\cdot|$ are the L_1 norm and the absolute value operators. $\mathbb{E}[\cdot]$ is the expected value and the natural logarithm $\log(\cdot)$ are used. Finally, $\cup$ denotes the union operator.

II. Capacity Bounds of Amplitude Constrained Interference Channels

In this section, we present two simple closed-form capacity bounds for a scalar Gaussian interference channel with amplitude constraints on the input signal and the interferences. Such a Gaussian interference channel with K interference sources is characterized by

$$Y = X + \sum_{i=1}^{K} I_i + N, \tag{1}$$

where X, I_i, N, Y denote the channel input, the $i-$th interference source, the noise, and channel output, respectively. The input X and the interference I_i are assumed to be constrained between $[-A, A]$ and $[-B_i, B_i]$, respectively, for some arbitrary positive values A, B_i. The noise random variable N is assumed to be Gaussian with zero mean and variance N_0. It is well known that without the interference terms, i.e., scalar Gaussian channel with amplitude input signal constraint only, the capacity-achieving distribution of X is unique and discrete with finite number of mass points [28]. However, the characterization of the capacity-achieving distribution for the channel

in (1) still remains an open problem. In what follows, a simple lower and upper capacity bounds are derived as benchmarks for optimal ZF precoder designs in the later part of the paper.

A. Lower Bound

The channel capacity of (1) is defined as

$$\begin{aligned} C &= \max_{f_X(x)} \ \mathbb{I}(X;Y) \\ &= \max_{f_X(x)} \ h(Y) - h(Y|X) \\ &= \max_{f_X(x)} \ h\left(X + \sum_{i=1}^{K} I_i + N\right) - h\left(\sum_{i=1}^{K} I_i + N\right) \end{aligned} \tag{2}$$

Using the Entropy Power Inequality (EPI) and the inequality $h(Q) \leq \frac{1}{2}\log 2\pi e\sigma_Q^2$ for a random variable Q with its variance σ_Q^2, a lower bound of C is given by

$$C_L = \frac{1}{2}\max_{f_X(x), f_{I_i}(i_i)} \log\left(e^{2h(X)} + \sum_{i=1}^{K} e^{2h(I_i)} + e^{2h(N)}\right) - \frac{1}{2}\log 2\pi e\left(\sum_{i=1}^{K}\sigma_{I_i}^2 + N_0\right) \tag{3}$$

According to the maximum entropy probability distribution, the uniform distribution is the maximum entropy probability distribution for a random variable under no constraint other than it is contained in the distribution's support [29]. In order to make the bound as tight as possible, it is reasonable to assume that X and I_i are uniformly distributed over $[-A, A]$ and $[-B_i, B_i]$, resulting in

$$\begin{aligned} C_L &= \frac{1}{2}\log\left(4A^2 + 4\sum_{i=1}^{K} B_i^2 + 2\pi e N_0\right) - \frac{1}{2}\log 2\pi e\left(\frac{\sum_{i=1}^{K} B_i^2}{3} + N_0\right) \\ &= \frac{1}{2}\log\frac{2\left(A^2 + \sum_{i=1}^{K} B_i^2\right) + \pi e N_0}{\pi e\left(\frac{\sum_{i=1}^{K} B_i^2}{3} + N_0\right)}. \end{aligned} \tag{4}$$

It is straightforward to see that, without interferences, the above bound reduces to a lower bound [16, Eq. (3)] as

$$C_L^o = \frac{1}{2}\log\left(1 + \frac{2A^2}{\pi e N_0}\right). \tag{5}$$

B. Upper Bound

Using the above mentioned entropy inequalities, an upper bound of C can be obtained from (2) by

$$C_U = \frac{1}{2}\log 2\pi e\left(\sigma_X^2 + \sum_{i=1}^{K}\sigma_{I_i}^2 + N_0\right) - \frac{1}{2}\max_{f_{I_i}(i_i)} \log\left(\sum_{i=1}^{K} e^{2h(I_i)} + e^{2h(N)}\right). \tag{6}$$

Similar to the case of the lower bound, assume that X and I_i are uniformly distributed over $[-A, A]$ and $[-B_i, B_i]$, respectively. As a result, C_U is given by

$$\begin{aligned} C_U &= \frac{1}{2}\log 2\pi e\left(\frac{A^2+\sum_{i=1}^K B_i^2}{3}+N_0\right)-\frac{1}{2}\log\left(4\sum_{i=1}^K B_i^2+2\pi e N_0\right) \\ &= \frac{1}{2}\log\frac{\pi e\left(\frac{A^2+\sum_{i=1}^K B_i^2}{3}+N_0\right)}{2\left(\sum_{i=1}^K B_i^2\right)+\pi e N_0}. \end{aligned} \tag{7}$$

Without interference, the above upper bound reduces to

$$C_U^o = \frac{1}{2}\log\left(1+\frac{A^2}{3N_0}\right). \tag{8}$$

C. Numerical Example and Asymptotic Behaviors

Figure 1 shows the lower and upper capacity bounds of the amplitude constrained interference channels for $K = 2$ with different levels of interference power. It can be seen that the gap between the lower and upper bounds is relatively small in the case of no interference. Specifically, it is straightforward to see that

$$\lim_{\frac{A}{\sqrt{N_0}}\to 0}(C_U^o - C_L^o) = 0, \tag{9}$$

and

$$\lim_{\frac{A}{\sqrt{N_0}}\to \infty}(C_U^o - C_L^o) = \frac{1}{2}\log\left(\frac{\pi e}{6}\right) \approx 0.1765 \text{ nats}. \tag{10}$$

In general, let us assume that the interferences are proportional to the input power, i.e., $B_i = \alpha_i A$ for some $\alpha_i > 0$. This assumption is generally valid in multi-user broadcast systems, where the interferences seen by a user are the transmitted signals for other users. Therefore, we can prove following asymptotic properties

$$\lim_{\frac{A}{\sqrt{N_0}}\to 0}(C_U - C_L) = 0, \tag{11}$$

and,

$$\lim_{\frac{A}{\sqrt{N_0}}\to \infty}(C_U - C_L) = \log\left(\frac{\pi e}{6}\right) \approx 0.353 \text{ nats}, \tag{12}$$

which are constant regardless of the interference power.

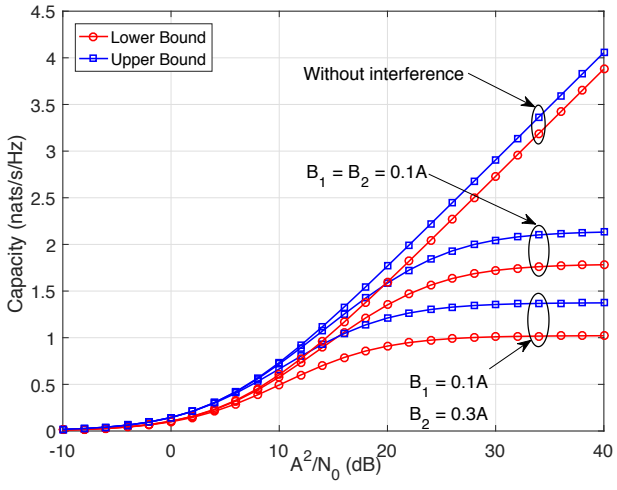

Figure 1: Lower and upper capacity bounds of amplitude constrained interference channels.

III. Multi-cell VLC Network Model

We consider multi-user multi-cell CoMP VLC broadcast networks consisting of M cells ($M > 1$) whose the primary purpose is the illumination of large areas. Each cell is formed by N_T LED arrays, which jointly serve K users [2] simultaneously by means of precoding techniques; and it is assumed that all signal processing is done by a central processing unit (CPU). Fig. 2a illustrates a 4-cell VLC network, where $N_T = 4$ and LED arrays are arranged in a rectangular shape. Wired connections, such as Ethernet, fiber or power-line communications, can be used between CPUs for inter-cell cooperation as well as cells to/from gateway transmissions. As the primary purpose of the system is illumination, a proper lighting design is required to provide an uniform illumination over the target plane. Therefore, it is inevitable that there are overlapping illuminated areas, which are referred as inter-cell interference areas, at the edges of each cell as shown in Fig. 2b.

We assume that each user is equipped with a single-photodiode (PD) receiver. Therefore, each cell can be essentially regarded as a multi-user (MU) MISO broadcast system. In such a multi-user broadcast system, the dominant performance-limiting factor is the multi-user interference (also known as intra-cell interference in the context of multi-cell networks). To alleviate the

[2]For mathematical descriptions, it is assumed that the number of users is the same for every cell. For numerical simulations, however, we also examine the case that cells have different numbers of users.

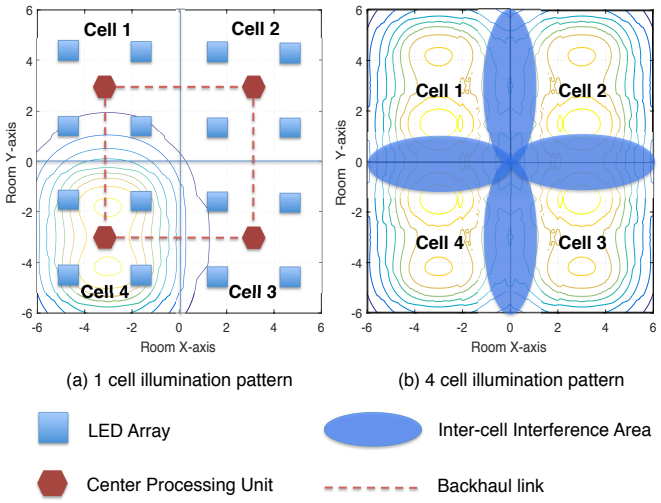

Figure 2: Multi-user multi-cell VLC network and illumination area.

impact of the intra-cell interference, different linear precoding schemes were considered and optimally solved under the unique constraints of visible light signal [15]–[17]. This paper, as we mentioned, deals with the multi-cell configuration, where, in addition to the intra-cell interference, the desired signals for users in one cell are also affected by by the signals for users of the adjacent cells, i.e., inter-cell interference. For the sake of notation, throughout the paper, we denote $\mathcal{N}_c = \{N_{c,1}, N_{c,2}, \ldots, N_{c,N_T}\}$ be the set of N_T LED arrays which belong to the $c-$th cell and $\mathcal{U}_c = \{U_{c,1}, U_{c,2}, \ldots, U_{c,K}\}$ be the set of K users located in this cell. It is also assumed that $N_T \geq K$.

A. *VLC Channel Model*

In case of indoor VLC, light signals from LED transmitters reach the receiver through multiple propagation paths due to reflection off the walls. As a consequence, the channel response is a summation of the light-of-sight (LoS) component and multiple non-light-of-sight (NLoS) ones. As pointed out in [25], the LoS component is dominant over the NLoS ones as it accounts for more than 95% of the total received optical power at the receiver. Moreover, even the strongest NLoS component is still at least 7 dB lower than the strongest LoS one [27]. To simplify the analyses, we thus consider the LoS channel only in this paper. Let $h_{c,i,k,j}$ be the LoS channel coefficient between the $i-$th LED array $N_{c,i}$ of the $c-$th cell and the $j-$th user $U_{k,j}$ of the $k-$th cell. In practice, most LED sources have Lambertian beam distribution, where the emission

intensity is given by

$$L(\phi_{c,i}) = \frac{l+1}{2\pi}\cos^{l}(\phi_{c,i}), \tag{13}$$

with $\phi_{c,i}$ is the angle of irradiance and l is the order of Lambertian emission determined by the semi-angle for half illuminance of the LED $\Phi_{1/2}$ as $l = -\frac{\log(2)}{\log(\Phi_{1/2})}$. For the most considered light-of-sight (LOS) link, $h_{c,i,k,j}$ is given [25]

$$h_{c,i,k,j} = \begin{cases} \frac{A_r}{r^2_{c,i,k,j}} L(\phi_{c,i}) T_s(\psi_{k,j}) g(\psi_{c,i,k,j}) \cos(\psi_{c,i,k,j}) & , 0 \leq \psi_{c,i,k,j} \leq \Psi, \\ & \\ 0 & , \psi_{c,i,k,j} > \Psi, \end{cases}, \tag{14}$$

where A_r and $r_{c,i,k,j}$ are the active area of the PD and the distance from the LED array to the user, respectively. Ψ denotes the optical FOV of the PD, $\psi_{c,i,k,j}$ is the angle of incidence and $T_s(\psi_{k,j})$ is the gain of the optical filter whereas $g(\psi_{c,i,k,j})$ is the gain of the optical concentrator and given by

$$g(\psi_{c,i,k,j}) = \begin{cases} \frac{\kappa^2}{\sin^2 \Psi} & , 0 \leq \psi_{c,i,k,j} \leq \Psi, \\ & \\ 0 & , \psi_{c,i,k,j} > \Psi, \end{cases} \tag{15}$$

where κ is the refractive index of the concentrator.

B. Precoding Model and Broadcast Transmission

In this study, we assume the use of pulse amplitude modulation (PAM) and let $d_{c,i} \in \mathbb{R}$ be the PAM data symbol that is intended to user $U_{c,i}$, $\mathbf{d}_c = \begin{bmatrix} d_{c,1} & d_{c,2} & \dots & d_{c,K} \end{bmatrix}^T \in \mathbb{R}^{K\times 1}$ be the data vector for all users of the $c-$th cell. Suppose that $d_{c,i}$ is zero mean and normalized to the range of $[-1, 1]$. At the LED array $N_{c,i}$, the broadcast signal $s_{c,i}$ for users of $\mathcal{U}_c$ is generated from a linear combination of the data vector and the matrix $\mathbf{V}_{c,i} = \begin{bmatrix} w_{c,i,1} & w_{c,i,2} & \dots & w_{c,i,K} \end{bmatrix} \in \mathbb{R}^{1\times K}$ as

$$s_{c,i} = \mathbf{V}_{c,i}\mathbf{d}_c. \tag{16}$$

Since $s_{c,i}$ can take on a negative value, which is not valid for the intensity modulation/direct detection (IM/DD) used in optical communications, a DC-bias $I^{\text{DC}}_{c,i}$ should be added to $s_{c,i}$ to ensure the non-negativity of the input signal, i.e.,

$$x_{c,i} = s_{c,i} + I^{\text{DC}}_{c,i} \geq 0. \tag{17}$$

As $\mathbb{E}[\mathbf{d}_c] = \mathbf{0}$, the signal $s_{c,i}$ does not effect the average illumination level of the LEDs. Instead, it is uniquely determined by the DC-bias $I_{c,i}^{\text{DC}}$. If we define $\mathbf{P}_c^s = \begin{bmatrix} P_{c,1}^s & P_{c,2}^s & \dots & P_{c,N_T}^s \end{bmatrix}^T \in \mathbb{R}^{N_T \times 1}$ is the transmitted power vector for the LED arrays of the $c-$th cell whose element $P_{c,i}^s = \eta x_{c,i}$ is the transmitted optical power of the $k-$th LED array with η being the LED conversion factor, the received optical signal at user $U_{c,k}$ can be written as

$$P_{c,k}^r = \begin{bmatrix} \mathbf{H}_{1,c,k} & \mathbf{H}_{2,c,k} & \dots & \mathbf{H}_{M,c,k} \end{bmatrix} \begin{bmatrix} \mathbf{P}_1^s & \mathbf{P}_2^s & \dots & \mathbf{P}_M^s \end{bmatrix}^T \tag{18}$$

where $\mathbf{H}_{i,c,k} = \begin{bmatrix} h_{i,1,c,k} & h_{i,2,c,k} & \dots & h_{i,N_T,c,k} \end{bmatrix} \in \mathbb{R}^{1 \times N_T}$ is the channel matrices between $\mathcal{N}_i$ and $U_{c,k}$.

If we denote $\mathbf{x}_c = \begin{bmatrix} x_{c,1} & x_{c,2} & \dots & x_{c,N_T} \end{bmatrix}^T \in \mathbb{R}^{N_T \times 1}$ as the transmitted signal vector and $\mathbf{I}_c^{\text{DC}} = \begin{bmatrix} I_{c,1}^{\text{DC}} & I_{c,2}^{\text{DC}} & \dots & I_{c,N_T}^{\text{DC}} \end{bmatrix}^T \in \mathbb{R}^{N_T \times 1}$ as the aggregated DC bias vector for users at the $c-$th cell, the received electrical signal at user $U_{c,k}$, after the optical-electrical conversion, is given by

$$\begin{aligned} y_{c,k} =& \gamma P_r^{c,k} + n_{c,k} = \gamma\eta \begin{bmatrix} \mathbf{H}_{1,c,k} & \mathbf{H}_{2,c,k} & \dots & \mathbf{H}_{M,c,k} \end{bmatrix} \begin{bmatrix} \mathbf{x_1} & \mathbf{x_2} & \dots & \mathbf{x_M} \end{bmatrix}^T + n_{c,k} \\ =& \gamma\eta \left(\mathbf{H}_{c,c,k}\mathbf{W}_{c,k}d_{c,k} + \underbrace{\mathbf{H}_{c,c,k} \sum_{i \in \mathcal{U}_c, i \neq k} \mathbf{W}_{c,i}d_{c,i}}_{\text{intra-cell interference}} + \underbrace{\sum_{c' \neq c} \sum_{j \in \mathcal{U}_{c'}} \mathbf{H}_{c',c,k}\mathbf{W}_{c',j}d_{c',j}}_{\text{inter-cell interference}} + \underbrace{\sum_{i=1}^{M} \mathbf{H}_{i,c,k}\mathbf{I}_{\text{DC}}^i}_{\text{DC current}} \right) \\ &+ n_{c,k}, \end{aligned} \tag{19}$$

with γ being the PD responsivity and $\mathbf{W}_{c,k} = \begin{bmatrix} w_{c,1,k} & w_{c,2,k} & \dots & w_{c,N_T,k} \end{bmatrix}^T \in \mathbb{R}^{N_T \times 1}$ being the *precoder* for user $U_{c,k}$. As seen from Eq. (19), the first term $\mathbf{H}_{c,c,k}\mathbf{W}_{c,k}d_{c,k}$ is the desired signal, the second and the third terms $\mathbf{H}_{c,c,k} \sum_{i \in \mathcal{U}_c, i \neq k} \mathbf{W}_{c,i}d_{c,i}$, $\sum_{c' \neq c} \sum_{j \in \mathcal{U}_{c'}} \mathbf{H}_{c',c,k}\mathbf{W}_{c',j}d_{c',j}$ represent the intra-cell and inter-cell interferences, respectively. $\sum_{i=1}^{M} \mathbf{H}_{i,c,k}\mathbf{I}_i^{\text{DC}}$ is the DC current that carries no data, $n_{c,k}$ denotes the receiver noise, which is assumed to be additive white Gaussian noise (AWGN) with zero mean and variance $\sigma_{c,k}^2$, given by [26], [27]

$$\sigma_{c,k}^2 = 2\gamma e \overline{P_{c,k}^r} B + 4\pi e A_r \gamma \chi_{\text{amp}} \left(1 - \cos\left(\Psi\right)\right) B + i_{\text{amp}}^2 B, \tag{20}$$

where e is the elementary charge, B denotes the system bandwidth and $\overline{P_{c,k}^r} = \mathbb{E}[P_{c,k}^r] = \eta \left(\sum_{i=1}^{M} \mathbf{H}_{i,c,k}\mathbf{I}_i^{\text{DC}} \right)$ is the average received optical power at user $U_{c,k}$. i_{amp} is the pre-amplifier noise current density, which comprises thermal noise and shot noise. χ_{amp} is the ambient light

photocurrent. After removing the DC current by AC coupling, the received signal can be written by

$$y_{c,k} = \gamma\eta\left(\mathbf{H}_{c,c,k}\mathbf{W}_{c,k}d_{c,k} + \mathbf{H}_{c,c,k}\sum_{i\in\mathcal{U}_c, i\neq k}\mathbf{W}_{c,i}d_{c,i} + \sum_{c'\neq c}\sum_{j\in\mathcal{U}_{c'}}\mathbf{H}_{c',c,k}\mathbf{W}_{c',j}d_{c',j}\right) + n_{c,k}. \quad (21)$$

C. ZF Precoding and Optical Power Constraint

As seen from Eq. (21), the desired signal of user $U_{c,k}$ can be greatly degraded by the inter-cell and the intra-cell interferences where the latter is generally more severe since it comes from the signals intended to users in the same cell which are stronger than that from the other cells. The intra-cell interference, however, can be effectively suppressed by utilizing ZF precoding technique whose idea is to construct the precoder $\mathbf{W}_{c,i}$ in such a way that it is orthogonal to $\mathbf{H}_{c,c,k}$, i.e.,

$$\mathbf{H}_{c,c,k}\mathbf{W}_{c,i} = 0 \;\; \forall i \in \mathcal{U}_c, i \neq k. \quad (22)$$

If we define $\mathbf{H}_c = \begin{bmatrix}\mathbf{H}_{c,c,1}^T & \mathbf{H}_{c,c,2}^T & \dots & \mathbf{H}_{c,c,K}^T\end{bmatrix}^T$ and $\mathbf{W}_c = \begin{bmatrix}\mathbf{W}_{c,1} & \mathbf{W}_{c,2} & \dots & \mathbf{W}_{c,K}\end{bmatrix}$, the ZF constraint in (22) implies that

$$\mathbf{H}_c\mathbf{W}_c = \begin{bmatrix}\sqrt{q_{c,1}} & & & \\ & \sqrt{q_{c,2}} & & \\ & & \ddots & \\ & & & \sqrt{q_{c,K}}\end{bmatrix} = \text{diag}\{\sqrt{\mathbf{q}_c}\}, \quad (23)$$

where $\sqrt{\mathbf{q}_c} = \begin{bmatrix}\sqrt{q}_{c,1} & \sqrt{q}_{c,2} & \dots & \sqrt{q}_{c,K}\end{bmatrix}^T$ whose $i-$th element represents the channel gain of user $U_{c,k}$.

With the constraint in (22), the received signal at $U_{c,k}$ is rewritten as

$$y_{c,k} = \gamma\eta\left(\mathbf{H}_{c,c,k}\mathbf{W}_{c,k}d_{c,k} + \sum_{c'\neq c}\sum_{j\in\mathcal{U}_{c'}}\mathbf{H}_{c',c,k}\mathbf{W}_{c',j}d_{c',j}\right) + n_{c,k}, \quad (24)$$

which contains the inter-cell interference term only. In addition to the ZF constraint in (22), one always must take the transmit power constraint into consideration when formulating optimal precoding designs. Fundamentally different from RF, the input current signal of the LEDs is non-negative and is amplitude constrained to a certain threshold, i.e., $0 \leq x_{c,i} \leq I_{\text{max}}$ with I_{max} being the maximum input current for the LEDs to maintain their linear operating range. Since

$d_{c,i}$ is assumed to be normalized within $[-1,1]$, these two constraints lead to the following constraint on the precoder design

$$\sum_{k=1}^{K} \left\| \left[\mathbf{W}_{c,k}\right]_{i,:} \right\|_1 \leq \Delta_{c,i}, \tag{25}$$

where $\Delta_{c,i} = \min\left(I_{c,i}^{\text{DC}}, I_{\max} - I_{c,i}^{\text{DC}}\right)$ [16].

In the following section, we investigate different cell coordination/cooperation strategies to mitigate the impact of the inter-cell interference. With respect to the derived lower and upper capacity bounds in Section II, the optimal coordinated/cooperative ZF precoding to maximize the users' sum-rate is then designed for each strategy accordingly.

IV. Cell Coordination/Cooperation Strategies

A. Per-Cell Coordinated Precoding

We first examine the simplest cell coordination level where all signal processing are performed on a per-cell basis. Nonetheless, cell coordination by sharing precoding designs are allowed. That is each cell deigns its own precoders taking into account the precoders of other cells. Following (4) and (7), the lower and upper capacity bounds of user $U_{c,k}$ are respectively given by

$$C_{c,k}^{L} = \frac{1}{2}\log\left(\frac{2(\gamma\eta)^2\left(\left(\mathbf{H}_{c,c,k}\mathbf{W}_{c,k}\right)^2 + \sum_{c'\neq c}\sum_{j\in\mathcal{U}_{c'}}\left(\mathbf{H}_{c',c,k}\mathbf{W}_{c',j}\right)^2\right) + \pi e\sigma_{c,k}^2}{\pi e\left(\frac{(\gamma\eta)^2\sum_{c'\neq c}\sum_{j\in\mathcal{U}_{c'}}\left(\mathbf{H}_{c',c,k}\mathbf{W}_{c',j}\right)^2}{3} + \sigma_{c,k}^2\right)}\right), \tag{26}$$

and

$$C_{c,k}^{U} = \frac{1}{2}\log\left(\frac{\pi e\left(\frac{(\gamma\eta)^2\left(\left(\mathbf{H}_{c,c,k}\mathbf{W}_{c,k}\right)^2 + \sum_{c'\neq c}\sum_{j\in\mathcal{U}_{c'}}\left(\mathbf{H}_{c',c,k}\mathbf{W}_{c',j}\right)^2\right)}{3} + \sigma_{c,k}^2\right)}{2(\gamma\eta)^2\sum_{c'\neq c}\sum_{j\in\mathcal{U}_{c'}}\left(\mathbf{H}_{c',c,k}\mathbf{W}_{c',j}\right)^2 + \pi e\sigma_{c,k}^2}\right). \tag{27}$$

In this coordinated scheme, the goal is to design precoders, i.e., $\mathbf{W}_{c,k}$, to maximize the lower and upper sum-rate (sum-capacity) of all users in the $c-$th cell. Moreover, it is straightforward to see that the optimal precoders to the problem of maximizing the lower sum-rate is the same

with that of the upper bound. Therefore, finding the optimal solution to maximize the lower sum-rate is sufficient.

$$\begin{aligned}
&\mathcal{P}\mathbf{1}: \\
&\underset{\mathbf{W}_{c,k}}{\text{maximize}} \quad \sum_{k=1}^{K} C_{c,k}^{L} \\
&\text{subject to} \quad \mathbf{H}_{c,c,k}\mathbf{W}_{c,i} = 0 \ \forall\, k \neq i, \\
&\qquad\qquad \sum_{k=1}^{K} \left\| \left[\mathbf{W}_{c,k}\right]_{i,:} \right\|_1 \leq \Delta_{c,i}.
\end{aligned} \tag{28}$$

It is important to note that, different from the single-cell setting, the choice of precoders at each cell affects the inter-cell interference at the neighboring cells, and that, in turn also affects their precoding design. As a result, the optimal solution to $\mathcal{P}\mathbf{1}$ needs to be found in an iterative manner until the sum-rate of each cell achieves its maximal value. Specifically for the $c-$th cell, at each iteration, we solve $\mathcal{P}\mathbf{1}$ to find $\mathbf{W}_{c,k}$ while all other $(M-1)K$ precoders $\mathbf{W}_{c',j}$ are fixed, i.e., the inter-cell interference term $\sum_{c'\neq c}\sum_{j\in\mathcal{U}_{c'}} \left(\mathbf{H}_{c',c,k}\mathbf{W}_{c',j}\right)^2$ is constant. However, even fixing the inter-cell interference, it can be seen that $\mathcal{P}\mathbf{1}$ is not a convex optimization problem due to the non-convexity of the objective function. Thus, it is generally difficult to find its optimal solution.

In our previous study, we developed an iterative algorithm based on the convex-concave procedure (CCCP) to find a local optimal solution to a problem which has the same form with $\mathcal{P}\mathbf{1}$. We redescribe the algorithm here for the sake of convenience. First, let us denote $\theta_{c,k} = \sum_{c'\neq c}\sum_{j\in\mathcal{U}_{c'}} \left(\mathbf{H}_{c',c,k}\mathbf{W}_{c',j}\right)^2$. By introducing a slack variable $\lambda_{c,k}$ and expressing $\mathbf{H}_{c,k}\mathbf{W}_{c,k} = \sqrt{q_{c,k}}$, $\mathcal{P}\mathbf{1}$ is then rewritten as

$$\begin{aligned}
&\mathcal{P}\mathbf{2}: \\
&\underset{\mathbf{W}_{c,k},q_{c,k},\lambda_{c,k}}{\text{maximize}} \quad \frac{1}{2}\sum_{k=1}^{K} \log\left(\frac{2\left(\gamma\eta\right)^2\left(\lambda_{c,k}+\theta_{c,k}\right)+\pi e\sigma_{c,k}^2}{\pi e\left(\frac{(\gamma\eta)^2\theta_{c,k}}{3}+\sigma_{c,k}^2\right)}\right) \\
&\text{subject to} \quad \mathbf{H}_c\mathbf{W}_c = \text{diag}\left\{\left[\sqrt{q_{c,1}} \quad \sqrt{q_{c,2}} \quad \cdots \quad \sqrt{q_{c,K}}\right]\right\}, \\
&\qquad \sum_{k=1}^{K} \left\| \left[\mathbf{W}_{c,k}\right]_{i,:} \right\|_1 \leq \Delta_{c,i}, \\
&\qquad q_{c,k} \geq \lambda_{c,k}, \\
&\qquad q_{c,k} \geq 0.
\end{aligned} \tag{29}$$

The objective function of $\mathcal{P}\mathbf{2}$ is now concave, yet the first constraint is not convex since $\mathbf{H}_c\mathbf{W}_c$ is affine while diag$\left\{\left[\sqrt{q_{c,1}} \quad \sqrt{q_{c,2}} \quad \dots \quad \sqrt{q_{c,K}}\right]\right\}$ is concave. The CCCP involves an iterative process to find a local maximal of $\mathcal{P}\mathbf{2}$ by, at the $i-$th iteration of the procedure, approximately linearizing the concave term $\sqrt{q_{c,k}^{(i)}}$ by its Taylor expansion as $\sqrt{q_{c,k}^{(i)}} \approx \sqrt{q_{c,k}^{(i-1)}} + \frac{1}{2\sqrt{q_{c,k}^{(i-1)}}}\left(q_{c,k}^{(i)} - q_{c,k}^{(i-1)}\right)$ where $q_{c,k}^{(i-1)}$ is the obtained from the previous iteration. From this approximation, $\mathcal{P}\mathbf{2}$ is transformed to a convex optimization problem which can be solved efficiently by using standard optimization packages. Capitalizing on the process for solving $\mathcal{P}\mathbf{2}$, we are now able to develop an iterative algorithm for solving $\mathcal{P}\mathbf{1}$ as follows

Algorithm 1 Iterative algorithm for solving problem $\mathcal{P}\mathbf{1}$

1: **Initialization**

1) Estimate channel matrices $\mathbf{H}_{c,c,k}$ and noise variances $\sigma_{c,k}^2$.

2) Initialize $\mathbf{W}_{c',k}^{(0)}$ to satisfy the constraint in (25).

2: **Iteration**: At the $i-$th iteration

1) Given $\mathbf{W}_{c',k}^{(i-1)}$, solve $\mathcal{P}\mathbf{2}$ using CCCP to find the optimal $\mathbf{W}_{c,k}^{(i)}$, denoted as $\mathbf{W}_{c,k}^{*(i)}$.

2) Use the obtained $\mathbf{W}_{c,k}^{*(i)}$ to solve $\mathcal{P}\mathbf{2}$ for other cells.

3) $i = i + 1$.

3: **Termination**: terminate the iteration when

1) $|\mathbf{W}_{c,k}^{(*i)} - \mathbf{W}_{c,k}^{*(i-1)}| \leq \epsilon$, where $\epsilon = 10^{-3}$ is a predefined threshold, or

2) $i = L$, where $L = 10$ is the predefined maximum number of iterations.

B. Coordinated Precoding

As can be seen from (24), the inter-cell interference can be problematic, especially for cell-edge users and in the case of populous cells. In the per-cell coordinated scheme, each cell designs precoders for its own users considering the interferences from other cells. The inter-cell interference, therefore, is minimized but not completely eliminated. From this observation, a natural way to cancel out the inter-cell interference is to *extend* the ZF precoder design in such a way that it takes into account the channels of users in other cells. This requires, for every cell, the availability of out-of-cell users' CSI through CSI sharing among cells. Different from

the per-cell coordinated scheme, once the inter-cell interference is eliminated, maximizing the sum-rate of users in all cells reduces to maximizing the sum-rate of users in each individual cell. With respect to the lower bound capacity from (5), the optimal precoding design is then formulated as

$$\begin{aligned}
&\mathcal{P}\mathbf{3}: \\
&\underset{\mathbf{W}_{c,k}}{\text{maximize}} \quad \sum_{k=1}^{K} \log\left(1+\frac{2(\gamma\eta)^2\mathbf{H}_{c,c,k}\mathbf{W}_{c,k}\mathbf{W}_{c,k}^T\mathbf{H}_{c,c,k}^T}{\pi e\sigma_{c,k}^2}\right) \\
&\text{subject to} \quad \mathbf{H}_{c,c,k}\mathbf{W}_{c,i}=0 \;\; \forall\, k\neq i, \{k,i\}\in\mathcal{U}_c \\
&\qquad\qquad \mathbf{H}_{c,c',k}\mathbf{W}_{c,i}=0 \;\; \forall\, c'\neq c, \; \forall\, k\in\mathcal{U}_{c'} \\
&\qquad\qquad \sum_{k=1}^{K}\left\|\left[\mathbf{W}_{c,k}\right]_{n,:}\right\|_1 \leq \Delta_{c,n}, \; \forall\, n=1,2,\cdots,N_T.
\end{aligned} \tag{30}$$

Although the second ZF constraint in $\mathcal{P}\mathbf{3}$ reduces the degrees of freedom on designing $\mathbf{W}_{c,k}$, it essentially removes the inter-cell interference introducing to users in other cells, thus significantly improve the overall sum-rate performance. Similar to problem $\mathcal{P}\mathbf{1}$, the above problem can be solved using the CCCP.

It should be noted that $\mathcal{P}\mathbf{3}$ is not always feasible. To see this, let $\overline{\mathbf{H}}_c=\left[\mathbf{H}_{c,c',k}^T\right]_{\forall c'\neq c,\forall k\in\mathcal{U}_{c'}}^T$ and $\tilde{\mathbf{H}}_{c,k}=\begin{bmatrix}\mathbf{H}_{c,c,1}^T & \cdots & \mathbf{H}_{c,c,k-1}^T & \mathbf{H}_{c,c,k+1}^T & \cdots & \mathbf{H}_{c,c,K}^T\end{bmatrix}^T$. A non-zero solution for the precoder of $U_{c,k}$ requires that the null space of $\begin{bmatrix}\tilde{\mathbf{H}}_{c,k}^T & \overline{\mathbf{H}}_c^T\end{bmatrix}^T$ has a dimension greater than 0, which is satisfied when $N_T > \text{rank}\left(\begin{bmatrix}\tilde{\mathbf{H}}_{c,k}^T & \overline{\mathbf{H}}_c^T\end{bmatrix}^T\right)$. Thus, the feasibility of $\mathcal{P}\mathbf{3}$ is equivalent to the condition that $N_T > \max\left\{\text{rank}\left(\begin{bmatrix}\tilde{\mathbf{H}}_{c,k}^T & \overline{\mathbf{H}}_c^T\end{bmatrix}^T\right)\right\}_{\forall c,k}$. This, however, is not always possible when $\begin{bmatrix}\tilde{\mathbf{H}}_{c,k}^T & \overline{\mathbf{H}}_c^T\end{bmatrix}^T$ is full row rank and the number of its row is larger than or equal to N_T. As a consequence, to ensure the feasibility of $\mathcal{P}\mathbf{3}$, every cell should accommodate at most N_T users. Since the first ZF constraint always needs to be satisfied as the intra-cell interference is generally more severe than the inter-cell one, the number of out-of-cell users being taken into account for the precoder design of one cell is then (N_T-K). The problem now is how to select those (N_T-K) out-of-cell users to maximize the overall sum-rate performance. One can immediately realize that those users should be selected from different cells as their channel are more spatially uncorrelated. In this paper, as we consider the simplest 2-cell configuration for numerical results, out-of-cell users are chosen randomly for the sake of simplicity. Once the set of out-of-cell users is determined for every cell, the optimal precode design problem is

essentially the same as $\mathcal{P}\mathbf{1}$ with an additional ZF constraint for the selected out-of-cell users. The optimal solution can then be found by an iteration algorithm.

C. Partial Cooperative Precoding with Data Sharing

Despite the previous coordinated precoding design helps to overcome the problem of inter-cell interference, one can further improve the sum-rate performance by allowing data sharing among cells to enhance users' SNR. With this assumption, one can immediately think of a full cooperation among all cells, i.e., cells act as a large single cell. This type of cooperation is essentially equivalent to the MU-MISO VLC broadcast systems with MN_T LED arrays and MK users discussed in [33]–[35]. In the context of RF communications, this full cell cooperation is sometimes referred as *multi-cell processing (MCP)*. The MCP imposes further signal processing constraints on the precoding design, especially when there are more cells and large number of users and in case of multi-cell VLC systems it is not always effective. That is because of the following two reasons. Firstly, with a proper lighting design, the inter-cell interference at a given cell can only come from its neighboring cells. Consequently, data symbols for users in one cell should only be shared to the neighboring cells. Secondly, due to the limited FOV of the LEDs, the inter-cell interference is mainly caused by the cell-edge LED arrays of the neighboring cells. Therefore, sharing data to all LED arrays of the neighboring cells might not help to improve the performance much. From these two observations, in this work, we thus consider a partial cooperation strategy, which requires relatively lower complexity compared to the full cooperation approach. In this scheme, the data symbols for users in $\mathcal{N}_c$ is only shared to the cell-edge LED arrays of the neighboring cells, which contribute the majority of the inter-cell interference. Those selected LED arrays in the neighboring cells cooperate with $\mathcal{N}_c$ to form a new set of LED arrays denoted as $\mathcal{N}_{\bar{c}}$, which now transmits signal to the users in the $c-$th cell. Hence, there are possibly several LED arrays which serve users in different cells. For mathematical convenience, let us denote

1) $\overline{\mathcal{N}}_{c',c}$ be the set of the cell-edge LED arrays of the $c'-$th cell, which borders to the $c-$th cell. As a result, $\mathcal{N}_{\bar{c}} = \mathcal{N}_c \bigcup_{\forall c'} \overline{\mathcal{N}}_{c',c}$.
2) $\overline{\mathcal{N}}_c = \bigcup_{\forall c'} \overline{\mathcal{N}}_{c',c}$ be the set of the cell-edge LED arrays of all adjacent cells of the $c-$th cell.
3) $\mathbf{H}_{\bar{c},c,k}$ be the channel matrix from $\mathcal{N}_{\bar{c}}$ to user $U_{c,k}$.
4) $\mathbf{W}_{\bar{c},c,k}$ be the precoder for user $U_{c,k}$.

With these notations, the received signal at user $U_{c,k}$ can then be written as

$$y_{c,k} = \gamma\eta\left(\mathbf{H}_{\bar{c},c,k}\mathbf{W}_{\bar{c},c,k}d_{c,k} + \mathbf{H}_{\bar{c},c,k}\sum_{i\in U_c, i\neq k}\mathbf{W}_{\bar{c},c,i}d_{c,i} + \sum_{c'\neq c}\sum_{j\in U_{c'}}\mathbf{H}_{\overline{c'},c,k}\mathbf{W}_{\overline{c'},c,j}d_{c',j}\right) + n_{c,k}. \tag{31}$$

Since each LED array can transmit data to users of different cells, the power constraint in (25) needs to be reformulated. Assume that the LED array $N_{c,k}$ in the $c-$th cell is indexed as $N_{c',k_{c'}}$ in the neighboring $c'-$th cell. The LED power constraint is then written as

$$\sum_{i\in U_c}\left\|[\mathbf{W}_{\bar{c},c,i}]_{k,:}\right\|_1 + \sum_{c'}\sum_{i\in U_{c'}}\left\|\left[\mathbf{W}_{\overline{c'},c,i}\right]_{k_{c'},:}\right\|_1 \leq \Delta_{\bar{c},c,k}. \tag{32}$$

Assume also that the data sharing process is done through a backhaul link connecting cells with unlimited capacity and no delay constraints, the optimal ZF precoder design problem for this cooperative form is given by

$$\begin{aligned}
\underset{\mathbf{W}_{\bar{c},c,k}}{\text{maximize}} \quad & \sum_{c=1}^{M}\sum_{k\in U_c}\log\left(1+\frac{2(\gamma\eta)^2\mathbf{H}_{\bar{c},c,k}\mathbf{W}_{\bar{c},c,k}\mathbf{W}_{\bar{c},c,k}^T\mathbf{H}_{\bar{c},c,k}^T}{\pi e\sigma_{c,k}^2}\right) \\
\text{subject to} \quad & \mathbf{H}_{\bar{c},c,k}\mathbf{W}_{\bar{c},c,i} = 0 \ \ \forall\, k, i\in U_c,\, k\neq i, \\
& \mathbf{H}_{\bar{c},c',k}\mathbf{W}_{\bar{c},c,i} = 0 \ \ \forall\, c\neq c', k\in U_{c'}, i\in U_c \\
& \sum_{i\in U_c}\left\|[\mathbf{W}_{\bar{c},c,i}]_{k,:}\right\|_1 + \sum_{c'}\sum_{i\in U_{c'}}\left\|\left[\mathbf{W}_{\overline{c'},c,i}\right]_{k_{c'},:}\right\|_1 \leq \Delta_{\bar{c},c,k}.
\end{aligned} \tag{33}$$

It should be noted that selecting all LED arrays in $\mathcal{N}_{c'}$ which have LOS link to $U_{c,k}$ may not be optimum since a certain selection of LED arrays in $\mathcal{N}_{c'}$ will affect the precoder design for users in this cell. It, in turn, has an impact on the sum-rate performance. For the sake of conciseness, we leave the problem of optimally selecting LED arrays for a future investigation.

V. Numerical Results and Discussions

In this section, numerical results are presented to demonstrate the effectiveness of different cell cooperation strategies. For the sake of illustration, we consider a two-cell CoMP VLC network with two users in each cell as depicted in Fig. 3. Additionally, a Cartesian coordinate system whose origin is in the center of the ceiling is used for specifying the positions of users and the LED arrays. We assume that all users are placed on the same receive plane, which is 0.6 m above the floor. Unless otherwise noted, the parameters of the room, LED arrays and optical receivers are given in Table I.

Table I: Multi-Cell VLC System Parameters

Parameter	**Value**
Room and LED configurations	
Room Dimension (Length × Width × Height)	12 (m) × 6 (m) × 3 (m)
Number of LED arrays, M	8
LED array size	0.1 (m) × 0.1 (m)
Number of LED chips per array	36
LED array posistions	Array 1: (-4, -1.5, 0) Array 2: (-2, -1.5, 0) Array 3: (-2, 1.5, 0) Array 4: (-4, 1.5, 0) Array 5: (2, -1.5, 0) Array 6: (4, -1.5, 0) Array 7: (4, 1.5, 0) Array 8: (2, 1.5, 0)
LED bandwidth, B	20 MHz
LED beam angle, ϕ (LED Lambertian order is 1)	120°
LED conversion factor, η	0.44 W/A
Receiver photodetectors	
PD active area, A_r	1 cm^2
PD responsivity, γ	0.54 A/W
PD field of view (FOV), Ψ	60°
Optical filter gain, $T_s(\psi)$	1
Refractive index of the concentrator, κ	1.5
Other parameters	
Ambient light photocurrent, χ_{amp}	10.93 $\text{A}/(\text{m}^2 \cdot \text{Sr})$
Preamplifier noise current density, i_{amp}	5 $\text{pA}/\text{Hz}^{-1/2}$

Firstly, the benefit of cell coordination/cooperation in reducing the impact of inter-cell interference is illustrated. To do this, we examine the performance of each coordination/cooperation strategy with respect to a user's position while fixing other users' positions. Specifically, we fix

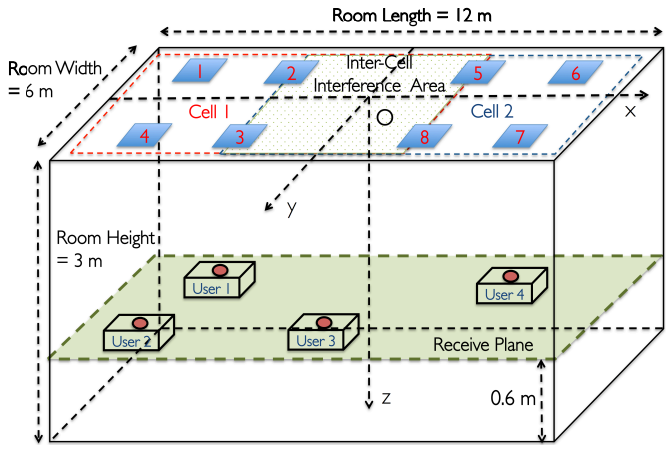

Figure 3: Geometrical configuration of a multi-user multi-cell MU-MISO VLC systems with 8 LEDs arrays.

the positions of User 1, 2, and 3 as follows

- User 1: UT1 $= \left(-3.2, \quad -1.8, \quad 2.4\right)$
- User 2: UT2 $= \left(-0.5, \quad 1.2, \quad 2.4\right)$
- User 3: UT3 $= \left(3.5, \quad -1.5, \quad 2.4\right)$

and let User 4 moves within Cell 2. Fig. 4 shows the lower bound maximum sum-rate performances of the considered schemes in accordance with User 4's position. The transmitted LED array power P_s is set to 35 dBm. The X-Y sweep resolution is $0.2(\mathrm{m}) \times 0.2(\mathrm{m})$. As clearly seen from the figure, the per-cell coordinated precoding suffers from poor performance especially when User 4 is in cell-edge area, i.e., the inter-cell interference area. On the other hand, the coordinated and partial cooperative schemes generally perform well as the inter-cell interference is effectively eliminated. Moreover, we also observe that the partial cooperative precoding offer a slightly better performance than the coordinated one does, especially when User 4 is close to either User 2 or User 3. That is because when users are close to each other, their channels become more correlated. The partial cooperative precoding with data sharing helps to improve users' received signal quality, thus reduce the impact of channel correlation.

Next, we present the averaged maximum sum-rate performance versus the average LED array transmitted power for the considered cooperative schemes with different numbers of users. All the results are obtained through 10,000 different channel realizations, i.e., 10,000 different positions

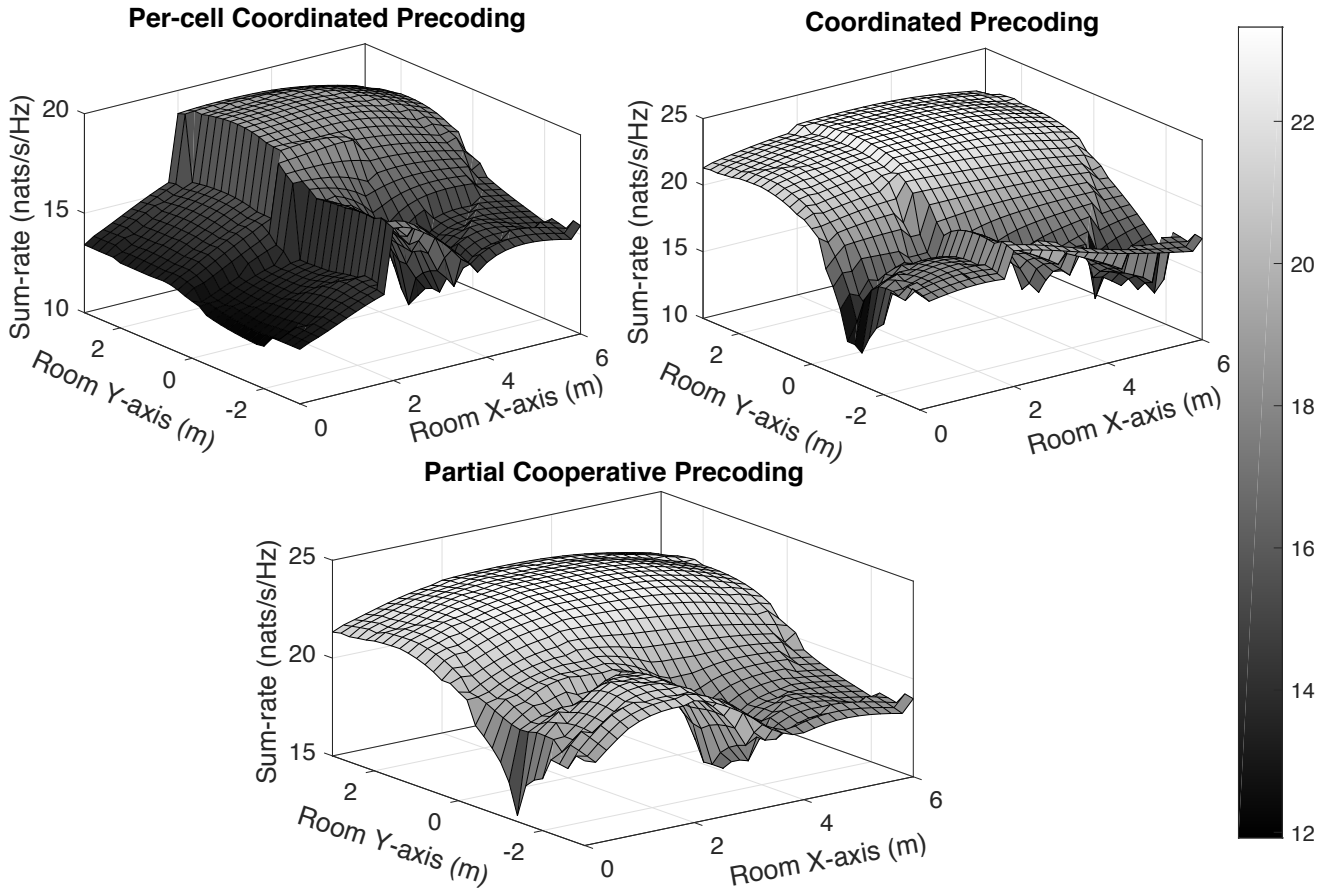

Figure 4: Maximum sum-rate distribution for different cooperative schemes.

of users uniformly located in their cell. First, we examine the case of having 4 users in total which corresponds to two different configurations: 2-by-2 (2 users in each cell) and 1-by-3 (1 users in the first cell and 3 users in the second cell). Figures 9 and 6 show the two cases of 2-by-2 and 1-by-3, respectively. The average LED array power ranges from 20 to 40 dBm, which corresponds from 0.1 to 10Watt. In both cases of user configuration, we observe significant performance improvements of the coordinated and partial cooperative precoding schemes over the per-cell coordinated one. Additionally, as the inter-cell interference is proportional to the LED transmitted power, these improvements increase in accordance with an increase in the LED transmitted power as well. Particularly, for both configuration at 40 dBm transmitted power, the performance gains of the coordinated and partial cooperative schemes are 5 and 6.2 nats, respectively. It is interesting to note that the partial cooperative precoding does not outperform the

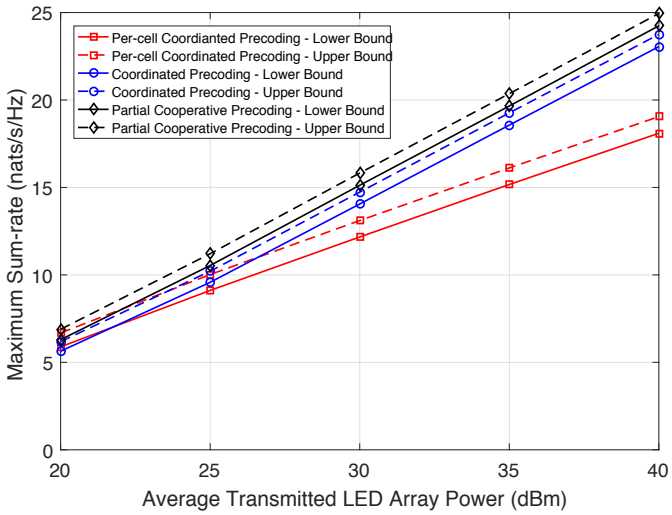

Figure 5: Average maximum sum-rate versus average LED array transmitted power: 2-by-2.

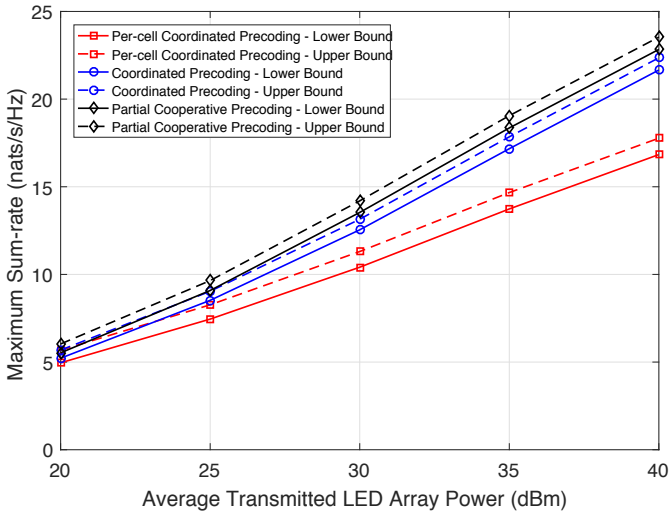

Figure 6: Average maximum sum-rate versus average LED array transmitted power:1-by-3.

coordinated scheme much, thus revealing that cell coordination without data sharing is sufficient enough to reduce the impact of inter-cell interference. Additionally, it is seen that the overall performance of the 2-by-2 configuration is slightly better than the 1-by-3 one. That is because with a relatively small number of LED arrays per cell, i.e., 4, the performance loss, on average, due to channel correlation in the 3-user-cell over the 2-user-cell is higher than that of 2-user-cell

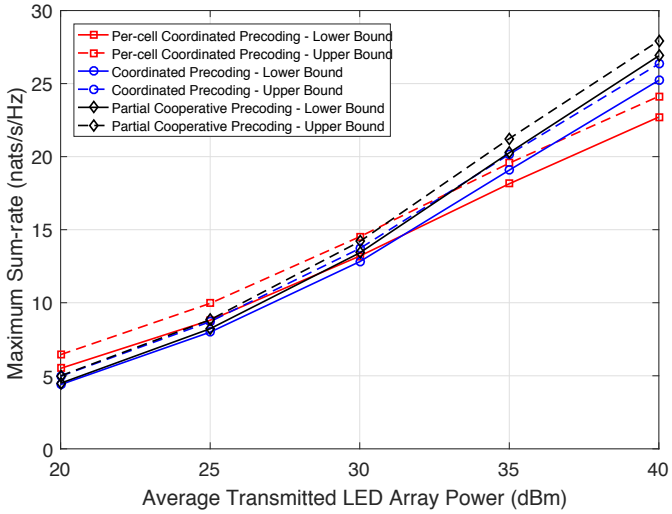

Figure 7: Average maximum sum-rate versus average LED array transmitted power: 3-by-3.

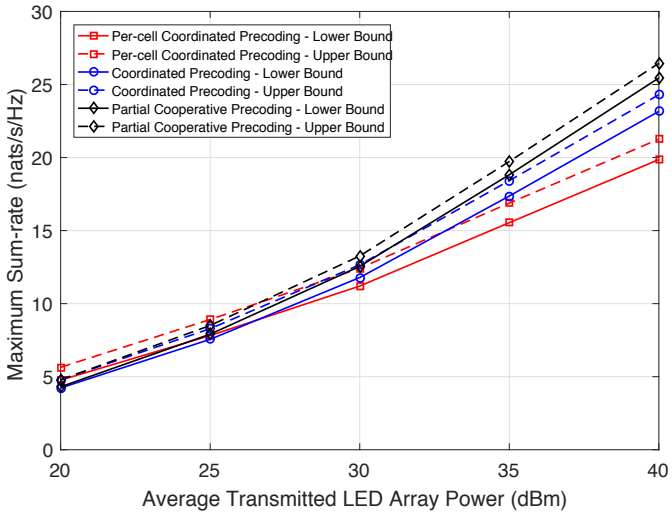

Figure 8: Average maximum sum-rate versus average LED array transmitted power: 2-by-4.

over the 1-user-cell.

In the case of more users per cell, Figs. 10 and 8 illustrate performances of 3-by-3 and 2-by-4 configurations, respectively. Compared to from the previous scenarios, the improvements of the coordinated precoding and partial cooperative precoding over the per-cell coordinated scheme are lower. At 40 dBm transmitted power, these improvements are 2.5, 4.2 nat in the

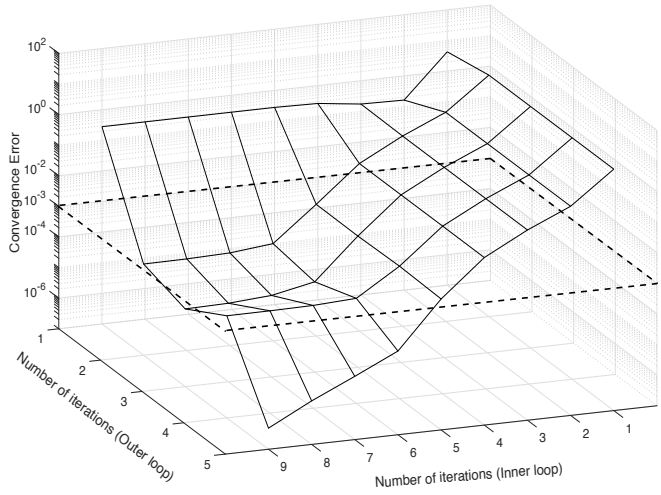

Figure 9: Convergence behavior of Algorithm 1: 2-by-2.

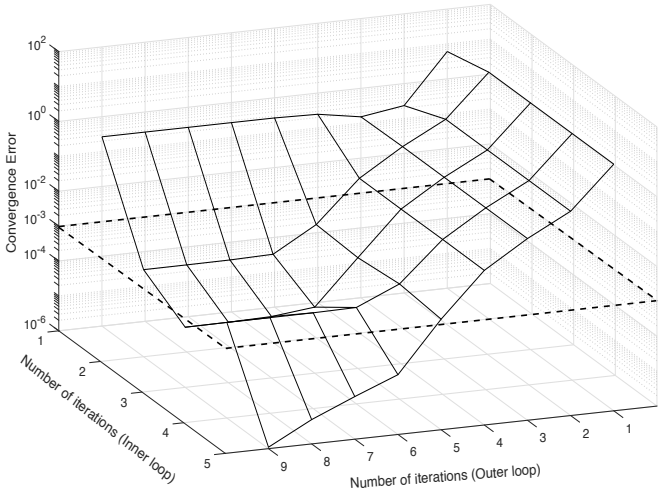

Figure 10: Convergence behavior of Algorithm 1: 3-by-3.

3-by-3 configuration and 3.3, 5.6 nat in the 2-by-4 one. Even at lower transmitted power, we observe that the per-cell coordinated scheme performs better than the two coordinated/cooperative schemes. The reason is when more users are involved in the coordinated/cooperative precoder designs (the number of uses per cell is large compared to the number of LED arrays per cell), the impact of channel correlation gets larger, i.e., there are less dimensions available for interference cancelation. Therefore, when the transmitted power is low the impact of the the

inter-cell interference, which is weak, is not as high as that of the channel correlation.

In Figs. 9 and 10, the convergence behaviors of Algorithm 1 for 2-by-2 and 3-by-3 scenarios are presented, respectively. The average LED array transmit power is set to 35 dBm. It should be noted that Algorithm 1 involves two iterative procedures, namely: an inner iterative loop to solve $\mathcal{P}2$ using CCCP and an outer iterative loop of the algorithm itself. In both cases, it is observed that at a target convergence error (i.e., convergence of the users' sum-rate) $\epsilon_{\text{convergence}} = 10^{-3}$, the algorithm requires on average 5 inner and 2 outer iterations, thus 10 iterations in total. As the speed of user's movement is typically slow in indoor scenarios, this low complexity of the algorithm confirms its practicality in case of time-varying VLC channels .

VI. Conclusions

In this paper, we have investigated several strategies of cell coordination/cooperation for a multi-user multi-cell CoMP VLC network. The optimal ZF precoder was designed to maximize the achievable sum-rate of users for each strategy. Numerical results showed that the partial cooperative precoding scheme, due to data sharing among cells, generally achieved the best performance while the coordinated precoding with less signal processing overhead also performed relative well. Interestingly, in the case when the number of users per cell is large compared to the number of LED arrays, the coordinated and partial cooperative precoding did not outperform much the per-cell coordinated precoding which even obtained better performance at lower transmitted power region.

References

[1] A. Jovicic, L. Junyi, T. Richardson, "Visible light communication: opportunities, challenges and the path to market," *IEEE Commun. Mag.*, vol. 51, no. 12, pp. 26–32, Dec. 2013.

[2] P. H. Pathak, X. Feng, P. Hu, and P. Mohapatra, "Visible light communication, networking, and sensing: a survey, potential and challenges," *IEEE Commun. Surveys Tuts.*, vol. 17, no. 4, pp. 2047–2077, Sept. 2015.

[3] D. Karunatilaka, F. Zafar, V. Kalavally, R. Parthiban, "LED based indoor visible light communications: state of the art," *IEEE Commun. Surveys Tuts.*, vol. 17, no. 3, pp. 1649–1678, Mar. 2015.

[4] A-M Cailean, M. Dimian, "Current challenges for visible light communications usage in vehicle applications: a survey," *IEEE Commun. Surveys Tuts.*, vol. 19, no. 4, pp. 2681–2703, May 2017.

[5] H. Ma, L. Lampe, S. Hranilovic, "Integration of indoor visible light and power line communication systems," in *Proc. of the IEEE International Symposium on Power Line Communications and Its Applications*, pp. 291–296, June 2013.

[6] X. Zhou and A. T. Campbell, "Visible light networking and sensing," in *Proc. of the ACM Workshop on HotWireless*, pp. 55–60, 2014.

[7] IEEE Std 802.15.7, IEEE Standard for Local and metropolitan area networks - Part 15.7: Short-range wireless optical communication using visible light, Mar. 2011.

[8] TG7r1, "Technical Considerations Document," doc: IEEE 802.15-15/0492r3, Sept. 2015, available: https://mentor.ieee.org/802.15/dcn/15/15-15-0492-03-007a-technical-considerations-document.docx.

[9] C. Chen, D. Tsonev, and H. Haas, "Joint transmission in indoor visible light communication downlink cellular networks," in *Proc. IEEE Global Communications Conference (GLOBECOM), Workshop on Optical Wireless Communications*, pp. 1127–1132, Dec. 2013,

[10] C. Chen, S. Videv, D. Tsonev, and H. Haas, "Fractional frequency reuse in DCO-OFDM-based optical attocell networks," *J. Lightw. Technol.,* vol. 33, no. 19, pp. 3986–4000, Oct. 2015.

[11] X. Li, R. Zhang, L. Hanzo, "Cooperative load balancing in hybrid visible light communications and wifi," *IEEE Trans. Commun.*, vol. 63, no. 4, pp. 1319–1329, Mar. 2015.

[12] B. G. Guzman, A. L. Serrano, V. P. G. Jimenez, "Cooperative optical wireless transmission for improving performance in indoor scenarios for visible light communications," *IEEE Trans. Consum. Electron.*, vol. 61, no. 4, pp. 393–401, Jan. 2016.

[13] Y. J. Zhu, W. Y. Wang, G. Xin, "Faster-than-Nyquist signal design for multiuser multicell indoor visible light communications," *IEEE Photon. J.*, vol. 8, no. 1, Feb. 2016, Art. ID 7902012.

[14] Z. G. Sun, H. Yu, Y. J. Zhu, "Efficient signal design and optimal power allocation for visible light communication attocell systems," *Appl. Opt.*, vol. 56, no. 32, pp. 8959–8968, Nov. 2017.

[15] H. Ma, L. Lampe, S. Hranilovic, "Coordinated broadcasting for multiuser indoor visible light communication systems," *IEEE Trans. Commun.*, vol. 63, no. 9, pp. 3313–3324, Sept. 2015.

[16] T. V. Pham, H. Le-Minh, A. T. Pham, "Multi-user visible light communication broadcast channels with zero-forcing precoding," *IEEE Trans. Commun.*, vol. 64, no. 6, pp. 2509–2521, June 2017.

[17] B. Li, J. Wang, R. Zhang, H. Shen, C. Zhao, L. Hanzo, "Multiuser MISO transceiver design for indoor downlink visible light communication under per-LED optical power constraints," *IEEE Photon. J.*, vol. 7, no. 4, Aug. 2015, Art. ID 7201415.

[18] S. Ma, R. Yang, H. Li, Z. L.Dong, H. Gu, S. Li, "Achievable rate with closed-form for SISO channel and broadcast channel in visible light communication networks," *J. Light. Technol.*, vol. 35, no. 14, pp. 2778–2787, July, 2017.

[19] J. Lian, M. B. Pearce, "Multiuser MIMO indoor visible light communication system using spatial multiplexing," *J. Light. Technol.*, vol. 35, no. 23, pp. 5024–5033, Oct. 2017.

[20] Z. G. Sun, H. Y. Yu, Z. J. Tian, Y. J. Zhu, "Linear precoding for MU-MISO VLC systems with noisy channel state information," *IEEE Commun. Lett.*, vol. 22, no. 4, pp. 732–735, Apr. 2018.

[21] X. Li, F. Jin, R. Zhang, J. Wang, Z. Xu, and L. Hanzo, "Users first: user-centric cluster formation for interference-mitigation in visible-light networks," in *IEEE Trans. Wireless Commun.*, vol. 15, no. 1, pp. 39–53, Jan. 2016.

[22] T. V. Pham, H. Le-Minh, A. T. Pham, "Multi-cell VLC: multi-user downlink capacity with coordinated precoding," in *Proc. of the IEEE Int. Conf. on Communications (ICC), Workshop on Optical Wireless Communications*, May 2017.

[23] T. V. Pham and Anh T. Pham, "Cooperation strategies and optimal precoding design for multi-user multi-cell VLC networks," in *Proc. of the IEEE Global Communications Conference (GLOBECOM)*, Dec. 2017.

[24] H. Ma, A. Mostafa, L. Lampe, S. Hranilovic, "Coordinated beamforming for downlink visible light communication networks," *IEEE Trans. Commun.*, vol. 66, no. 8, pp. 3571–3582, Aug. 2018.

[25] T. Komine, M. Nakagawa, "Fundamental analysis for visible-light communication system using LED lights," *IEEE Trans. Consum. Electron.*, vol. 50, no. 1, pp. 100–107, Feb. 2004.

[26] D. C. O'Brien, M. Katz, "Optical wireless communications within fourth-generation wireless systems," J. Optical Networking, vol. 4, no. 6, pp. 312–322, 2005.

[27] L. Zeng, D. C. O'Brien, H. L. Minh, G. E. Faulkner, K. Lee, D. Jung, Y. Oh, E. T. Won, "High data rate multiple input multiple output (MIMO) optical wireless communications using white LED lighting," *IEEE J. Sel. Areas Commun.*, vol. 27, no. 9, pp. 1654–1662, Dec. 2009.

[28] J. G. Smith, "The information capacity of amplitude and variance-constrained scalar Gaussian channels," *J. Inf. Control*, vol. 18, no. 3, pp. 203–219, Apr. 1971.

[29] T. Cover, J. Thomas, "Elements of information theory," *Wiley Inter-science*, 2006.

[30] L. Vandenberghe, S. Boyd, S. P. Wu, "Determinant maximization with linear matrix inequality constraints," *SIAM J. Matrix Anal. Appl.*, vol. 19, no. 2, pp. 499–533, Apr. 1998.

[31] M. Grant, S. Boyd, "CVX: Matlab software for disciplined convex programming version 2.1," *http://cvxr.com/cvx/*, Jan. 2015.

[32] J. Lofberg, "YALMIP : a toolbox for modeling and optimization in MATLAB," *IEEE Int. Symp. on Computer Aided Control Systems Design*, pp. 284–289, Sept. 2004.

[33] S. Chatzinotas, M. A. Imran, C. Tzaras, "Uplink capacity of MIMO cellular systems with multicell processing," in *Proc. of the IEEE International Symposium on Wireless Communication Systems*, Oct. 2008.

[34] H. Dai and H. Poor, "Asymptotic spectral efficiency of multicell MIMO systems with frequency-flat fading," *IEEE Trans. Signal Processing*, vol. 51, no. 11, pp. 2976–2988, Nov. 2003.

[35] S. Chatzinotas, M. A. Imran, R. Hoshyar, "On the multicell processing capacity of the cellular MIMO uplink channel in correlated rayleigh fading environment," *IEEE Trans. Wirel. Commun.*, vol. 8, no. 7, July 2009.